16th World Conference on Earthquake, 16WCEE 2017

Santiago Chile, January 9th to 13th 2017

Paper N° 4505

Registration Code: S-I1460539050

MAGNITUDE DEPENDENCE OF STRESS DROP: WHAT DOES THE OBSERVED MAGNITUDE SCALING OF GROUND-MOTIONS TELL US?

B. Derras[(1,2,3)], F. Cotton[(4,5)], S. Drouet[(6)], P-Y. Bard[(7)]

[(1)] *PhD student, ISTerre, University of Grenoble Alpe, Grenoble, France, boumediene.derras@univ-grenoble-alpes.fr.*
[(2)] *Researcher, RISAM laboratory, University of Tlemcen, Algeria, b_derras@mail.univ-tlemcen.dz.*
[(3)] *Associate Professor, University of Saïda, Algeria.*
[(4)] *Professor, Helmholtz Centre Potsdam, German Research Center for Geosciences (GFZ), Germany, fcotton@gfz-potsdam.de.*
[(5)] *Professor, Institute of Earth and Environmental Sciences, University of Potsdam, Germany.*
[(6)] *Researcher, Geoter International – FUGRO Group, Auriol, France, stephane@on.br.*
[(7)] *Professor, ISTerre, University of Grenoble Alpe, CNRS, IFSTAR, Grenoble, France, pierre-yves.bard@ univ-grenoble-alpes.fr.*

Abstract

The behavior of earthquake stress-drop magnitude scaling has been the topic of significant debate in the earthquake source community over the past two decades. Methodologies which have been adopted by a large number of source studies require corrections for source radiation pattern, path attenuation and site amplification that ultimately introduce large uncertainties for stress-drop estimates. In this study, we adopt a different strategy: we analyze directly the ground-motions (Y) and their dependencies with magnitude (M). We first use simple stochastic models (e.g. [1]) comprised of a [2, 3] source spectrum and various models of magnitude-dependent stress drop. We show that magnitude-dependent stress-drop and constant stress-drop models lead to different scaling of ground-motions (dlogY/dM) with frequency. Using the results of [4], we then analyze the magnitude dependency of NGA-West 2 ground-motions for source-site configurations where stress-drop is the key controlling factor of ground-motions (moderate distances and rock-sites). In addition, the use of a neural network method allows us to obtain fully record-driven evaluations of (dlogY/dM) with frequency both for simulated and observed records. The comparison between these observed and simulated (dlogY/dM) allows us to discuss the scaling of the stress-drop with magnitude. We do not observe strong differences of the magnitude scaling of ground-motions between mainshocks and aftershocks.

Keywords: Source scaling; ground motion; stochastic models; neural networks; stress drop

1. Introduction

Dynamic stress drop ("Brune" stress-drop) is a key parameter in the estimation of strong ground motion, as it influences the high-frequency level of acceleration ([2], [3]). There are many methods for simulating ground motion from earthquakes. Each has particular strengths, and each can provide estimates of ground motion. However, the simulation methods all depend, directly or indirectly, on the selected dynamic stress drop which is then a primary input parameter needed to compute ground-motion simulations (e.g. stochastic simulations).

Since the seminal work of [5], stress drops have been assumed to be constant, allowing for scaling between earthquakes of different magnitudes. However, several studies have suggested a magnitude-dependence of the Brune's stress-drop for Mw<4.5 [6, 7, 8]. Such results generate a large epistemic uncertainty and the inflation of hazard logic tree branches in regions where models based on small earthquakes have to be extrapolated to large earthquakes. There is then an urgent need to better constrain the magnitude scaling of stress-drops. However, classical methods to analysis stress drops are facing some practical and theoretical problems.

a) Brune's stress-drop evaluation is strongly dependent on the corner frequency measurements uncertainty and corner frequencies are difficult to measure (e.g. [9]).

b) Fourier spectra spectral inversion results may be biased by trade-off between source, path and site effects including kappa the high-frequency decay of ground-motion amplitude (e.g. [10]). Methodologies which have been adopted to analyze the behavior of earthquake source scaling require substantial corrections for path attenuation, site amplification, and source radiation pattern effects that ultimately yield large variances for corner frequency estimates and subsequently for stress-drop estimates [11].

c) Potential regional variations of source parameters and the heterogeneity of inversion methods complicate the analysis of stress-drops.

d) Spectral ratios of two co-located events removes common path and site effects, but this method implies the use of mainshocks and aftershocks of a single sequence.

In this study, we adopt a different strategy: we analyze directly the ground-motions (Y) and their dependencies with magnitude (M). Such analysis is performed both on data-driven empirical models data and physics-based, stochastic, models. Several authors (e.g. [12]) have already been comparing the magnitude scaling of ground-motions predicted both by empirical models and more physics based models. Such comparisons were limited because of the range of magnitude covered by classical crustal earthquakes GMPE's (the magnitude range of these models was usually between 4.5 and 7.5), the fact that classical GMPE's functional forms depend on developers a priori choices and also the difficulty to evaluate the relative impact of source, path and site effects on ground-motions. We then develop here a more comprehensive method to analyze the dependency of ground-motions on the stress-drop magnitude-scaling:

1. We first take advantage of the recent development of the NGA-West 2 database [13]. This database is now allowing the development of ground-motion models for magnitudes as low as 3.5. Only recordings from shallow crustal events are considered, including mainshocks as well as aftershocks.

2. We build synthetics ground-motions databases using stochastic simulations and various models of magnitude-dependent stress drop: three synthetic databases with $\Delta\tau$ = 2.5 Mpa, $\Delta\tau$ = 5 Mpa and $\Delta\tau$ = 10 Mpa (constant stress drop) and two databases based on [8] and [11] magnitude-dependent stress drop models.

3. We use the Artificial Neural Network (ANN) approach [14] to get fully data-driven empirical predictive models

4. We then analyze the magnitude dependency of NGA-West 2 ground-motions for source-site configurations where stress-drop is the key controlling factor of ground-motions accorading to the recent results of [4].

Finally, the comparison between these observed and simulated (dlogY/dM) allow us to discuss the scaling of the stress-drop with magnitude. We also compare the differences of the magnitude scaling of ground-motions between mainshocks and aftershocks.

2. Data

2.1 NGA-West 2 dataset

The NGA-West 2 project is a large multidisciplinary, research program on the Next Generation Attenuation (NGA) models for shallow crustal earthquakes in active tectonic regions. The flatfiles established by the project [13] contain site and source information, along with distances parameters and the corresponding ground-motion intensity measures (IMs). Only a subset of this database was used [15].

One of the aims of our study is to compare the magnitude scaling of ground-motion for both mainshock and the aftershock events. In the NGA-West 2 database, we use the definition of Class 1 and Class 2 events described in [16] to distinguish mainshocks and aftershocks.

2.2 Stochastic simulations of ground-motions (SSGM)

The stochastic simulations are based on the method of [8]. A set of stochastic parameters is considered, including uncertainties on each parameter. The uncertainty is then propagated through the simulations by random sampling of the parameters distributions. The SMSIM program [1] is used to simulate data for M_w from 3 to 8 at epicentral distances between 1 and 250 km. Virtual fault planes are created in order to compute various distance metrics and for each magnitude-epicentral distances pairs, a number of different configurations around the fault plane are simulated (various azimuths). The attenuation parameters considered are those [8], and standard rock site conditions are considered. A generic velocity profile from [17] with V_{s30}=800 m/s is used together with kappa= 0.03 s. Uncertainties on kappa and on the site amplifications computed from the velocity profile are propagated [8].

2.3 Data distribution

The distributions of the datasets according to M_w, R_{hyp}, and PSA are displayed on Fig.1. This figure illustrates the range of M_w =[3 to 6.5] and R_{hyp}< 60 km for NGA-West 2 and R_{hyp}<41.79 km for SSGM. To minimize the influence of site effects we use NGA-West 2 data with V_{s30}>500 m/s.

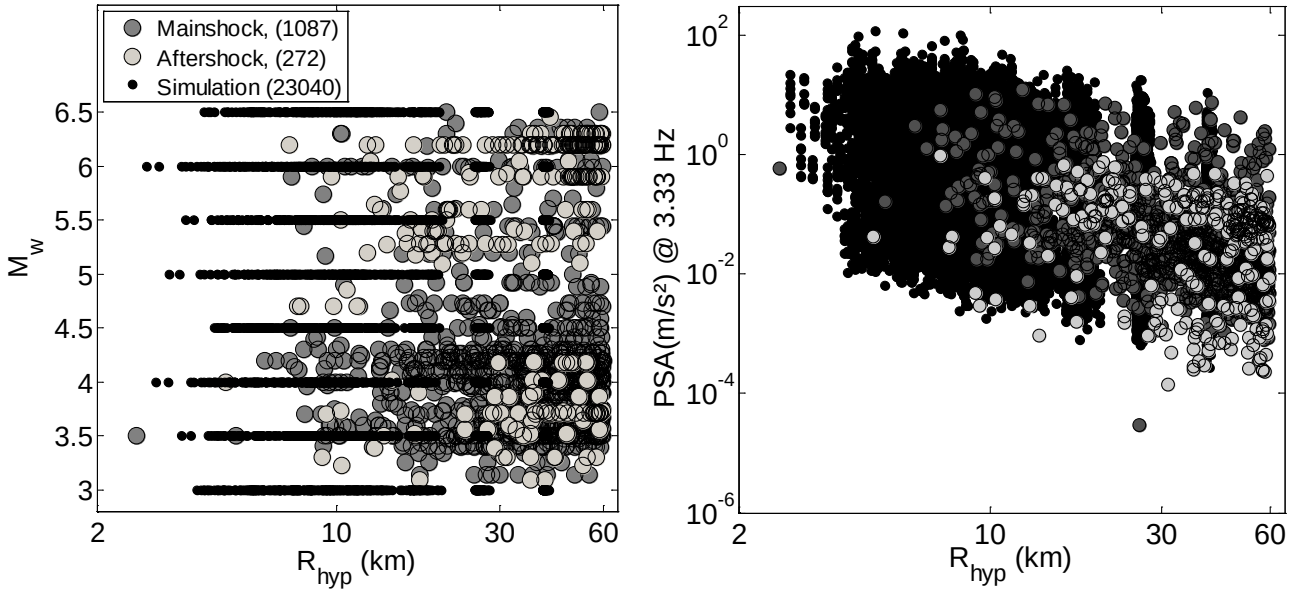

Fig. 1 - Distribution of the databases considered in this study in the [Magnitude (M_w) - distance (R_{hyp})] (left), [PSA @ 3.33 Hz - R_{hyp}] (right).

3. Method

3.1 Development of data-driven ground-motion models

The input parameters are M_w and R_{hyp}. The predicted ground-motions are the geometric mean of the horizontal components for PGA, PGV, and 5%-damped PSA at 19 frequencies from 0.33 to 100 Hz.

A feed-forward backpropagation neural network type is used. The structure of the ANN is displayed in Fig.2. This structure has been taken from [14]. The input and output layers contain the input and output parameters, and are linked through one single hidden layer consisting of only three neurons. This small number of neurons is the optimal hidden neurons number in order to optimize both the total sigma [9] and the Akaike Information Criterion [18]. The type of activation functions between input and hidden layers, and between hidden and output layers have been adopted after several tests [19]. It resulted in the choice of a "tangent sigmoïd" type for the hidden layer and a "linear" one for the output layer. The quasi-Newton Back Propagation technique has been applied for the training phase [20]. To avoid “over-fitting” problems we chose an adequate regularization method developed by [14] together with a limited number of neurons on the hidden layer. In Fig.2, the symbols W and b represent the synaptic weights and bias with subscripts representing the corresponding neurons between two layers.

At the end, eight different ANN models were built, differing by the dataset. For the eight datasets, the earthquakes are described by the moment magnitudes Mw and the source to site distances by R_{hyp} and site effect is not modeled (also explained below only sites with V_{s30}>500 m/s are considered here). The first ANN model is based on only mainshocks from the NGA-West 2 database and the second ANN relies on only aftershocks data. For the third ANN model all the NGA-West 2 data are considered (this model is the reference model for the comparison study). Using the synthetic data three ANN models are based on simulations for constant stress drop of 2.5, 5 and 10 Mpa, respectively, and two other ANN models are based on simulations for magnitude-dependent stress drop using the stress drop models of [11] and [8].

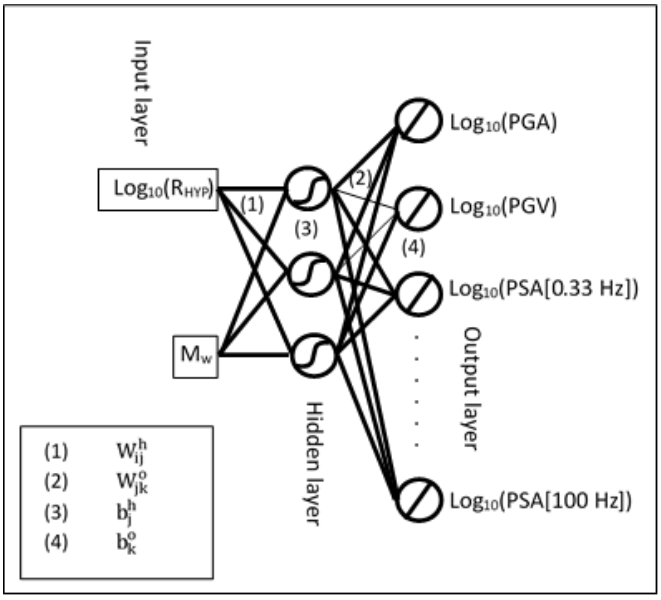

Fig. 2 - Structure of the Neural Networks considered for the prediction of PGA, PGV and PSA[0.33 to 100 Hz].

w_{ij}^h is the synaptic weight between the i[th] neuron of the input layer and the j[th] neuron in the hidden layer, b_j^h the

bias of the j[th] neuron in the hidden layer. Also the w_{jk}^{o} is the synaptic weight between the j[th] neuron of the hidden layer and the k[th] neuron in the output layer, b_{k}^{o} the bias of the k[th] neuron in the output layer

3.2 Optimal configuration to analyze the magnitude scaling

To analyze the influence of stress drop in ground-motion magnitude scaling, we shall minimize the influence of site effect, anelastic attenuation, kappa effect.

To limit site effect influence, NGA-West 2 data with V_{s30} (a widely used site effect proxy) greater than 500 m/s are selected. At first an even greater V_{s30} was used but this resulted in a too small number of data to derive ANN models. An important point is to choose the optimal frequency range to analyze the influence of stress drop on ground-motion magnitude scaling. [4] analyzed the sensitivity of response spectral amplitudes on seismological parameters using algorithmic differentiation. They found that at 2 to 7 Hz, there is a large impact of stress drop and a low impact of kappa, Q and M_w. Therefore, for this study, we select a frequency equal to 3.33 Hz for the stress-drop analyze.

[21] and [22] show that regional ground-motions variations start to be significant for distances greater than 60-70 km. To limit the impact of regional attenuation variations only data recorded at distances lower than 60 km have been selected. Fig.3 shows the magnitude scaling of ground-motions against M_w at a distance of 30 km. The choice of a different distance limit (40 and 30 km) for the data selection does not impact the observed magnitude scaling.

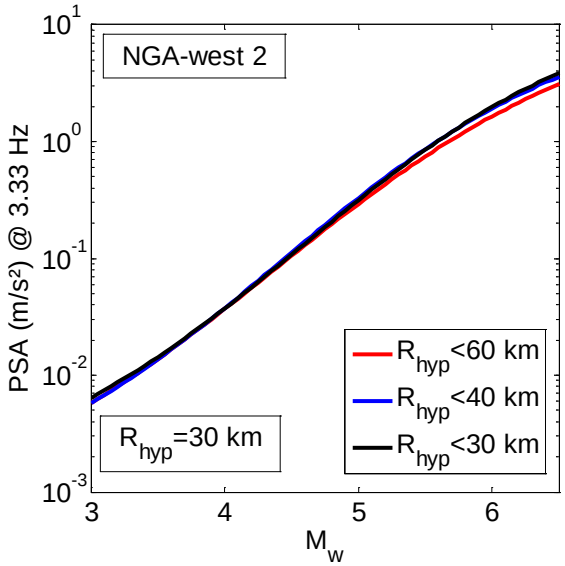

Fig. 3 - Magnitude-dependence of ANN models based on various data selection (R<30km, R<40km, R<60km)

3.3 Robustness of ANN approach

Tests of the robustness of the predicted ground-motion values were carried out using different subsets of the whole database to train the ANN. Fig.4 compares the pseudo-spectral acceleration curves vs M_w derived when using 100%, and 25% of the whole datasets. For each run, the records of the training set were selected randomly. The results are shown here for a target distance R_{hyp}=30 km (which falls in the area with a lot off data). This result shows that the ground-motion model derived using the ANN method and the NGA-West2 database is stable at a distance of 30 km.

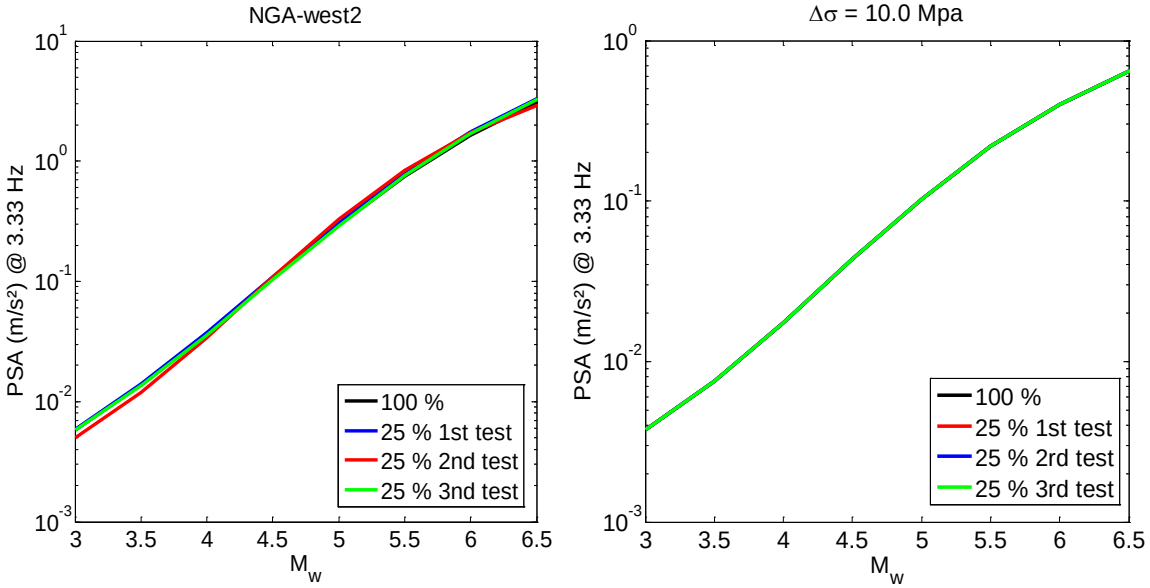

Fig. 4 - Robustness of the ground-motion scaling derived using the ANN approach and the NGA-West 2 dataset. The graphs show the relationship between PSA at 3.33 Hz and magnitude for various subsets of the database.

4. Results

4.1 Do aftershocks and mainshocks show a different ground-motion magnitude scaling?

Some previous studies, such as [23], have found that the median short-period ground motions from aftershocks are smaller than the median ground motions from mainshocks. In our study, the ANN predictive models derived with aftershocks and mainshocks data show the same ground-motion magnitude scaling. Again, some tests have been performed for various subsets of the NGA-West 2 database characterized by various maximum distances 30 km (Fig.5).

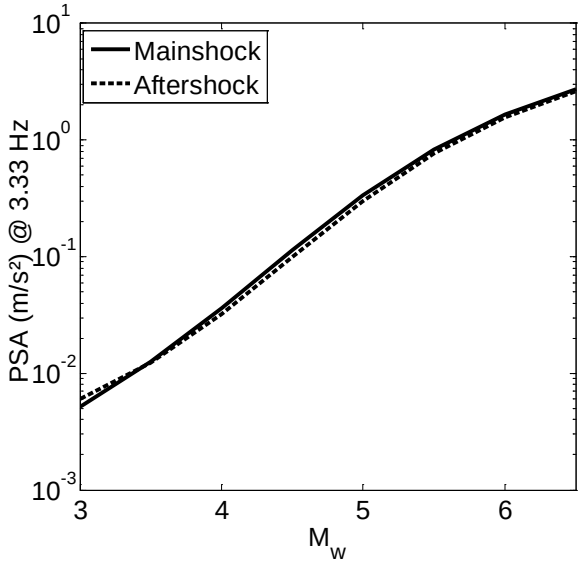

Fig. 5 - ANN predictive models derived with Aftershocks and Mainshocks data for 30 km.

4.2 Comparison between the magnitude scaling of observed (NGA-West 2) and simulated ground-motions

In the last section, we have found that the mainshocks and aftershocks show a similar ground-motion magnitude scaling. For this reason, we now use all NGA-west 2 (aftershocks and mainshocks) ground-motions to compare observed and simulated magnitude scalings.

First, we show the various Brune's stress drop models used in the stochastic simulations (Fig.6). Two types of models have been implemented: constant stress-drop models (10, 5 and 2.5 MPa) and magnitude-dependent models. The magnitude-dependent models have been taken from the studies of [8] and [11]. These models both suggest an increase of stress-drop with magnitude. The Drouet and Cotton model is based on the analysis of moderate stress-drops analysis in the French Alps. This model suggest a significant stress-drop increase from magnitude 3 to 4.5. The [11] model is suggesting a stress-drop increase from M=4.5 to M=5.5.

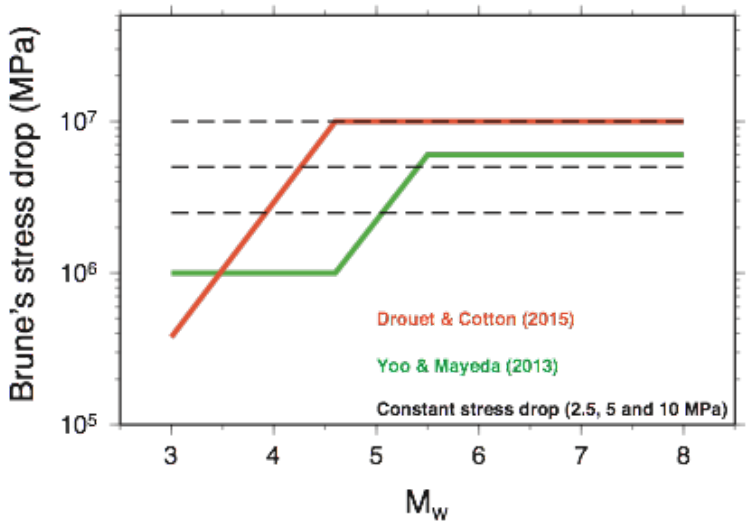

Fig. 6 - Stochastic simulations of ground-motions (SMSIM, [1]) with various stress-drop models

We then compare the observed NGA-West 2 ground-motion magnitude scaling and the scaling predicted by stochastic simulations performed with the stress-drop models shown on Fig.6. Fig.7a first illustrates the comparison with stochastic simulations performed with constant stress-drops models. None of the selected models is showing a perfect fit. The tests shows that the amplitude of the stress drops has an impact both on the slope and the amplitude of the scaling. The closest model is obtained for a constant stress-drop $\Delta\tau$=10 Mpa. All models underestimate the magnitude scaling (dlogY/dM) for low (M<4) and large (M>5) earthquakes. The tested magnitude dependent stress-drops do not show either a perfect fit. Fig.7 shows that the magnitude scaling of stress-drop has a strong impact on the slope of the ground-motion magnitude-scaling.

To illustrate this, ground-motion amplitudes have been normalized by the observed or predicted amplitude at M_w=4.5 and a distance of 30 km. The results (Fig.8) shows that the [11] model show an increase of the magnitude scaling which is similar to the observed one. However, given the fact that stress-drop amplitudes have an impact on the magnitude-scaling increase (Fig.7a) it is not straight forward to derive a model which will fit the relationship (amplitude and slope) between dlogY/dM and the magnitude.

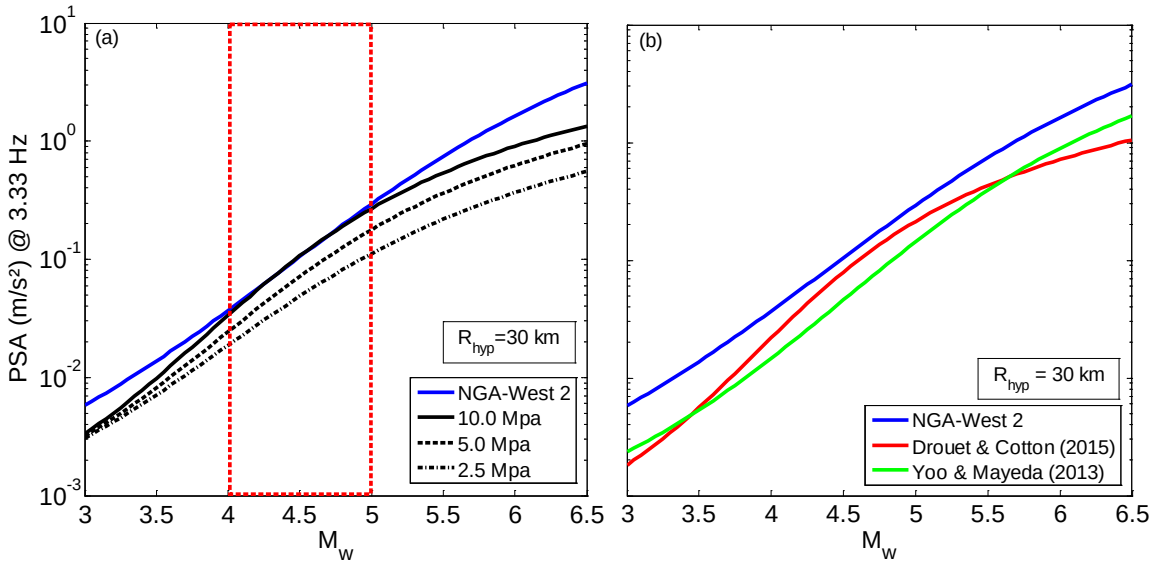

Fig. 7 - Comparison between the magnitude scaling of observed (NGA-West 2) and simulated ground-motions at the distance of 30 km.

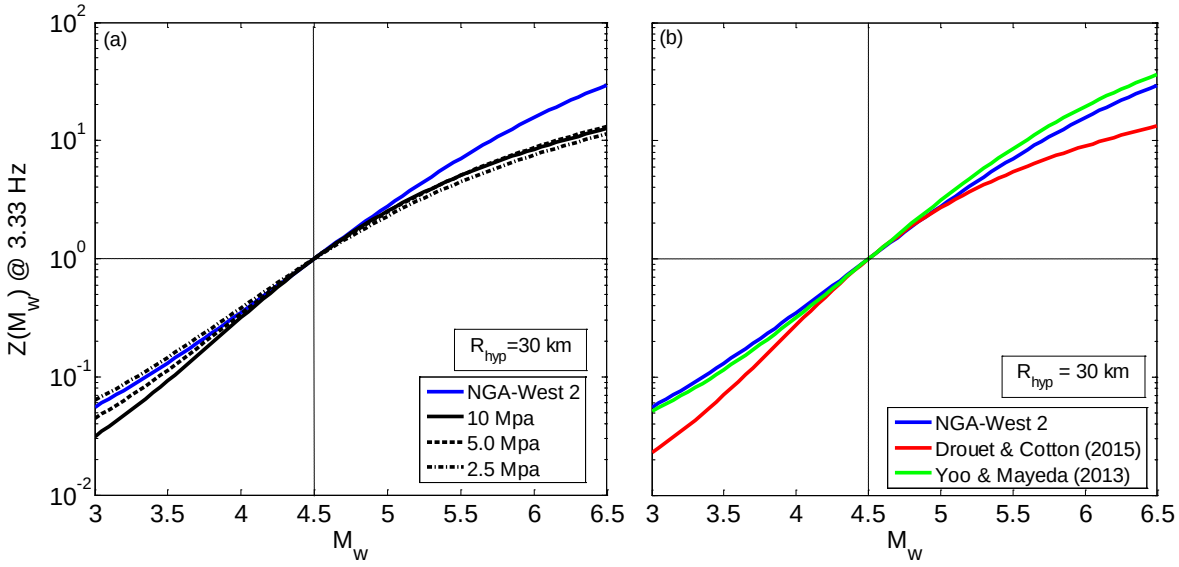

Fig. 8 - Magnitude-dependent decay of the seven models, for pseudo absolute acceleration spectra (PSA) at 3.3 Hz. We represent the ground-motion intensity normalized ($Z(M_w)$)at M_w=4.5 versus magnitude at the distance of 30 km

5. Conclusion

We first take advantage of the recent development of the NGA-West 2 database [13] to analyze the magnitude scaling (dlogY/dM) of ground-motions for shallow crustal earthquakes. We then analyze the magnitude dependency of NGA-West 2 ground-motions for source-site configurations (30 km, 3.3 Hz) where stress-drop is the key controlling factor of ground-motions. The comparison between these observed and simulated scaling (dlogY/dM) allows to discuss the scaling of the stress-drop with magnitude and compare the differences of the magnitude scaling of ground-motions between mainshocks and aftershocks. These results confirm that NGA-West 2 aftershocks and mainshocks ground-motions show a similar magnitude scaling. These tests also suggest that the relation-ship between stress-drops and ground-motion magnitude scaling is far to be linear. Constant

stress-drop models and the tested magnitude-dependent models have not been able so far to reproduce the observed scaling.

6. Acknowledgments

The authors would like to thank the participants of the NGA-West 2 program for providing high quality data and stimulating ideas.

7. Data and resources

The datasets used in this article have been collected and disseminated by The Pacific Earthquake Engineering Research Center.

8. References

[1] Boore DM (2003): Simulation of ground motion using the stochastic method, *Pure Appl. Geophy*, 160, 635–675.

[2] Brune JN (1970): Tectonic stress and the spectra of seismic shear waves from earthquakes, *J. Geophys. Res*, 75(26), 4997–5009, doi: 10.1029/JB075i026p04997.

[3] Brune JN, (1971): Correction to "Tectonic stress and the spectra, of seismic shear waves from earthquakes", *J. Geophys. Res*, 76, 5002.

[4] Molkenthin C, Scherbaum F, Griewank A, Kuehn N, Stafford P (2014): A study of the sensitivity of response spectral amplitudes on seismological parameters using algorithmic differentiation, Bull. Seismol. Soc. Am. 104, 2240–2252, doi: 10.1785/0120140022.

[5] Aki K (1967): Scaling law of seismic spectrum. *Journal of Geophysical Research*, 72, (4), 1217–1231

[6] Edwards B, Fäh D (2013): A stochastic ground-motion model for Switzerland, *Bull. Seismol. Soc. Am*, 103, 78–98.

[7] Rietbrock A, Strasser FO, Edwards B (2013). A stochastic earthquake ground-motion prediction model for the United Kingdom, Bull. Seismol. Soc. Am. 103, 57–77.

[8] Drouet S, Cotton F (2015): Regional Stochastic GMPEs in Low-Seismicity Areas: Scaling and Aleatory Variability Analysis—Application to the French Alps. *Bull. Seism. Soc. Am*, 105 (4), 1883–1902, doi: 10.1785/0120140240

[9] Cotton F, Archuleta R, Causse M (2013): What is sigma of the stress drop? *Seismol. Res. Lett*, 84, 42–48, doi: 10.1785/0220120087.

[10] Drouet S, Cotton F, P.Guéguen (2010): V_{S30}, κ, regional attenuation and M_w from small magnitude events accelerograms, *Geophys. J. Int*. 182, 880–898.

[11] Yoo SH, Mayeda K (2013): Validation of Non-Self-Similar Source Scaling Using Ground Motions from the 2008 Wells, Nevada, Earthquake Sequence. Bulletin of the Seismological Society of America, Vol. 103, No. 4, pp. 2508–2519, August 2013, doi: 10.1785/0120120327.

[12] Luco JE (1985): On strong ground-motion estimates based on models of the radiated spectrum. *Bull. Seism. Soc. Am*, 75 (3) 641-649.

[13] Ancheta TD, Darragh, RB, Stewart JP, Seyhan E, Silva WJ, Chiou B. S-J, Wooddell KE, Graves RW, Kottke AR, Boore DM, Kishida T, Donahue JL (2014): NGA-West 2 database, *Earthquake Spectra*, 30, 989–1005.

[14] Derras B, Bard P-Y, Cotton F, Bekkouche A (2012): Adapting the neural network. Approach to PGA prediction: an example based on the KiK-net data, *Bull. Seism. Soc. Am*, 102, 1446–1461.

[15] Derras B, Bard P-Y, Cotton F (2016): Site-conditions proxies, ground-motion variability and data-driven GMPEs. Insights from NGA-West 2 and RESORCE datasets. *Earthquake spectra*, doi: http://dx.doi.org/10.1193/060215EQS082M

[16] Wooddell KE, Abrahamson NA 2014: Classification of main shocks and aftershocks in the NGA-West 2 database, Earthquake Spectra 30, 1257–1267.

[17] Cotton F, Scherbaum F, Bommer JJ, Bungum H (2006): Criteria for selecting and adjusting ground-motion models for specific target regions: Application to Central Europe and rock sites, *J. Seismol*, 10, doi: 10.1007/s10950-005-9006-7.

[18] Akaike H (1973): Information theory and an extension of the maximum likelihood principle, in Proc. of the 2nd International Symposium on Information Theory, Budapest 1, 267–281.

[19] Derras B, Bard P-Y, and Cotton F, (2014): Towards fully data-driven ground-motion prediction models for Europe. *Bull. Earthq. Eng*, 12, 495-516.

[20] Shanno DF, Kettler PC (1970): Optimal Conditioning of Quasi-Newton Methods," Math. Comp 24, 657-664.

[21] Boore DM, Thompson EM (2014): Path durations for use in the stochastic-method simulation of ground motions, *Bull. Seismol. Soc. Am*, 104, 2541–2552, doi: 10.1785/0120140058.

[22] Kotha SR, Bindi D, Cotton F (2016): Partially non-ergodic region specific GMPE for Europe and Middle-East. - *Bulletin of Earthquake Engineering*, 14, 4, p. 1245-1263.

[23] Abrahamson NA, and Silva WJ (2008): Summary of the Abrahamson & Silva NGA ground motion relations, *Earthquake Spectra*, 24, 67–97.